Available online at www.sciencedirect.com

ScienceDirect

Energy Procedia 92 (2016) 326 – 335

Energy Procedia

6th International Conference on Silicon Photovoltaics, SiliconPV 2016

Corona charge in SiO_2: kinetics and surface passivation for high efficiency silicon solar cells

Ruy S Bonilla[a*], Nicolas Jennison[a], Deborah Clayton-Warwick[b], Katherine A Collett[a], Lucy Rands[a], Peter R Wilshaw[a]

[a]*Department of Materials, University of Oxford, Oxford, OX1 3PH , UK*
[b]*Department of Physics, University of California Santa Barbara, Santa Barbara, CA 93106, US*

Abstract

This manuscript presents a method by which capacitance-voltage measurements can be used in conjunction with Kelvin-probe measurements to calculate the location of charge within a dielectric layer. A first order kinetic model for the transport of charge into SiO_2 films after exposure to corona charge deposition is proposed. The rate limiting step for charge migration into oxide films has been observed to be the injection of charge from the surface (air-SiO_2 interface). The charge lies preferentially at the air-SiO_2 and SiO_2-Si interfaces, and its injection into SiO_2 has been characterized as having an activation energy of ~ 50 meV. In this work, corona charge deposition has produced SRV < 2.7 cm/s and J_{01} < 12 fA/cm^2 which is within the requirements of high efficiency silicon solar cells. These results contribute to the understanding of corona charge interaction with SiO_2 with a view to its potential application as an extrinsic method of passivation for highly efficient silicon solar cells.

Peer review by the scientific conference committee of SiliconPV 2016 under responsibility of PSE AG.

Keywords: silicon solar cells; surface passivation; field effect passivation; corona discharge; dielectric films.

1. Introduction

Corona discharge is a technique routinely used to deposit positive or negative charge on the surface of materials. When used on dielectric coatings on top of silicon, it provides the ability to control the semiconductor surface

* Corresponding author. Tel.: +44 1865 283097; fax: +44 1865 273789.
E-mail address: sebastian.bonilla@materials.ox.ac.uk

Peer review by the scientific conference committee of SiliconPV 2016 under responsibility of PSE AG.
doi:10.1016/j.egypro.2016.07.090

concentration of carriers and thus provide surface passivation by means of field effect [1]. Corona discharges have been largely used in research to characterize the electrical properties of silicon-dielectric interfaces [2]. Despite the fact that extremely effective passivation is possible (SRV< 2 cm/s) [3,4], the exploitation of corona charge for passivation of practical solar cells has been hindered by the lack of stability of the deposited charge [5,6]. Only recently, new reports on the stabilization of corona induced charge have suggested its eventual application at an industrial level [7,8]. For this to happen, a better understanding of the high temperature kinetic behavior of charge in dielectric films is required. Alongside this, a model to determine the position of charge within a dielectric layer is presented. This is vital in characterizing migration and stability of charge within dielectrics.

2. Experimental methods

Float-zone (FZ), 1 Ωcm, n-type silicon wafers were dry oxidized at 1050 ˚C to create a 100 nm SiO_2 coating. Wafers were then diced into either 1 x 1 cm^2 or 3 x 3 cm^2 specimens and subjected to a dehydration and Hexamethyldisilazane (HMDS) coating treatment at 130 ˚C. This treatment is designed to reduce both the concentration of water within the films, and to prevent water from being absorbed by the films [9]. This is necessary since charge leakage is known to occur due to the presence of water molecules and hydroxyl groups within or at the surface of the film [10,11]. Corona charge was deposited using a single point electrode held at 15 kV, 17 cm above the specimen. Kelvin-Probe (KP) backing potential [12] measurements were taken to measure surface charge of the specimens. Mercury probe (Hg-p) capacitance-voltage (CV) flat-band voltage measurements were conducted using a Boonton 7200 CV meter at 1 MHz using a set-up as illustrated in Fig. 1. Photoconductance decay lifetime measurements were taken using a Sinton Lifetime WCT-120 [13].

Nomenclature

ε_0	permitivity of free space (8.85 x10^{14}) [F/cm]
ε_i	permittivity of insulator [F/m]
E_a	activation energy [eV]
n	concentration of ions [cm^{-2}]
n_{ao}	concentration of ions at air-oxide interface [cm^{-2}]
n_{os}	concentration of ions at oxide-Si interface [cm^{-2}]
k	Boltzmann constant (8.617 x 10^{-5}) [eV/K]
K_i	relative permittivity of insulator
q	elementary charge (1.6 x 10^{-19}) [C]
Q_{CV}	charge per unit area at the dielectric-Si interface as measured by CV [q/cm^2]
Q_{KP}	charge per unit area at the dielectric-air interface as measured by KP [q/cm^2]
Q_{it}	interface trapped charge at the silicon surface [q/cm^2]
ρ_i	volumetric charge distribution [q/cm^3]
t_i	insulator thickness [nm]
T	temperature [K]
t	time [s]
Φ_{m}	metal work function [eV]
Φ_{ms}	metal to semiconductor work function difference [eV]
Φ_s	semiconductor work function [eV]
Φ_{sm}	semiconductor to metal work function difference [eV]
ϕ_{scr}	semiconductor surface potential due to the space charge region [V]
V_{bKP}	Kelvin probe backing potential [V]
V_{fb}	flat-band voltage from CV measurements [V]
V_g	potential at the gate [V]
ψ_i	potential difference produced by charge in insulator [V]
x_c	distance of charge centroid from insulator-Si interface [cm]

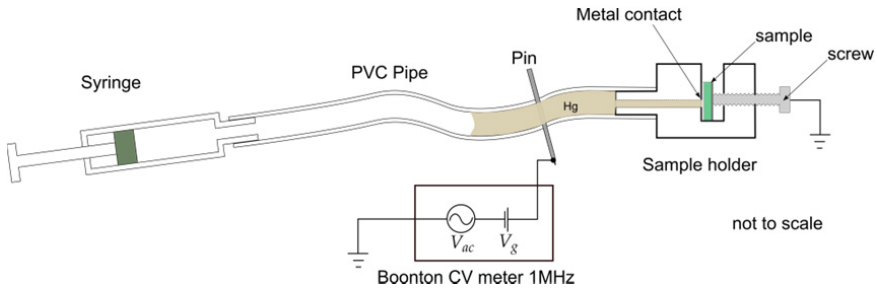

Fig. 1. Schematic of mercury probe capacitance-voltage set up.

3. Location of charge

In this section we draw the theoretical approach to estimate the concentration and centroid of charge within a dielectric from KP and CV measurements is outlined. KP backing potential and Hg-p CV flat-band measurements were made on the n-type Si samples previously described thus reproducing a metal-insulator-semiconductor (MIS) structure. Schematics of these two systems, band diagrams and example plots of charge, electric field and potential are shown in Fig. 2. It is important to note that the convention for the *x* axis follows the electrode that is used as the reference potential in each measurement; this is different in each case.

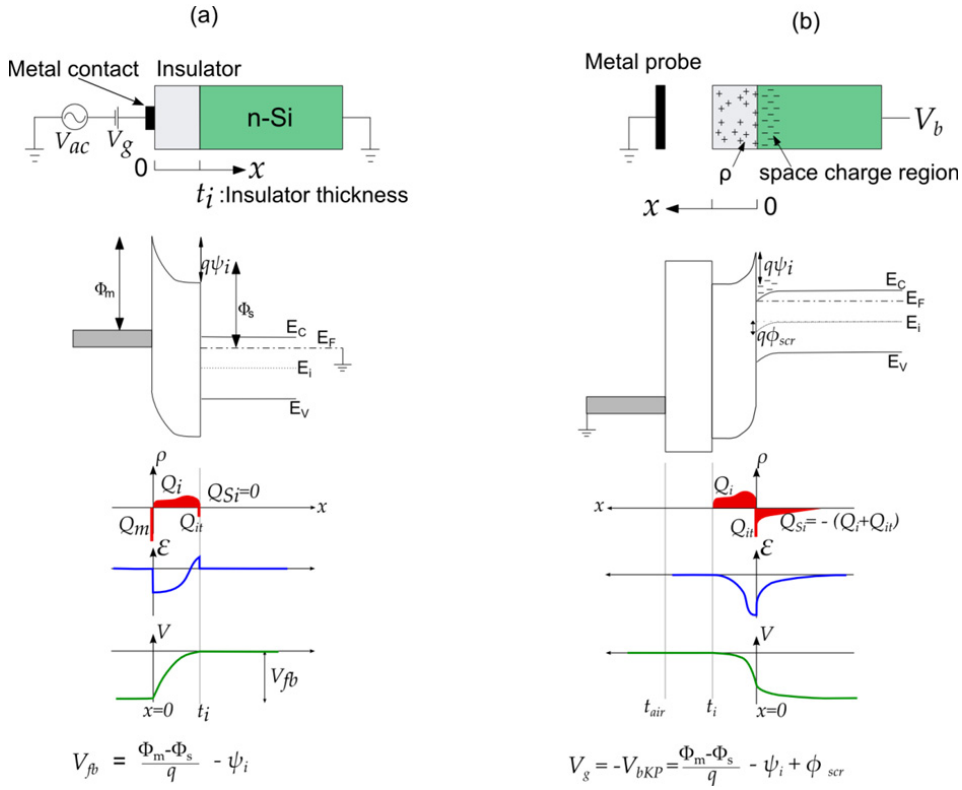

Fig. 2. Schematics of equipment set up, and example band diagrams, charge, electric field and potential traces for (a) CV and (b) KP measurements.

For CV measurements, it is well known that the gate voltage, with reference to the semiconductor, is given by [14]:

$$V_g = \frac{\Phi_{ms}}{q} - \psi_i + \phi_{scr} - \frac{Q_{Si}}{\varepsilon_i/t_i} \tag{1}$$

Where Φ_{ms} is the metal to semiconductor work-function difference, ϕ_{scr} the potential difference between the bulk and the surface of the semiconductor due to the space charge region, Q_{Si} is the silicon charge producing a potential drop across the insulator ($C_i = \varepsilon_{\mathrm{i}}/\mathrm{t_i}$) [15], and ψ_i is the potential drop due to charge in the insulator, including both its interface to the metal and to the semiconductor. ψ_i thus includes the potential drop due to the semiconductor interface trapped charge Q_{it}: $\psi_{it} = Q_{it}t_i/\varepsilon_i$. This interface trapped charge develops due to ionized acceptor and donor states at the insulator-semiconductor interface and is dependent on the semiconductor surface potential ϕ_{scr}. This leads to the well-known expression for flat-band voltage ($\phi_{scr} = 0$, $Q_{si} = 0$) in CV measurements [16]:

$$V_{fb} = \frac{\Phi_{ms}}{q} - \psi_i = \frac{\Phi_{ms}}{q} - \frac{Q_{it}(\phi_{scr}=0)t_i}{\varepsilon_i} - \frac{1}{\varepsilon_i}\int_0^{t_i} x\rho_i(x)dx \tag{2}$$

Where ψ_i has been split into potential arising from interface trapped charge, and that arising from a volumetric charge distribution $\rho_i(x)$ inside the insulator [17,18]. The insulator charge is often represented as a single sheet of charge concentration Q_i, given in units of C/cm^2, with centroid x_c from the insulator-silicon interface. The volumetric charge ρ can thus be expressed as a delta Dirac function centered at $t_i - x_c$: $\rho(x) = Q_i\,\delta(x - [t_i - x_c])$. In which case, the potential difference due to insulator charge is $Q_i(t_i - x_c)/\varepsilon_i$ and the flat-band voltage becomes:

$$V_{fb} = \frac{\Phi_{ms}}{q} - \frac{Q_{it}(\phi_{scr}=0)t_i}{\varepsilon_i} - \frac{Q_i(t_i - x_c)}{\varepsilon_i} \tag{3}$$

When the flat-band voltage is found in CV measurements, the inferred charge is commonly calculated as:

$$Q_{CV} = \frac{\varepsilon_i}{t_i - x_c}\left(\frac{\Phi_{msCV}}{q} - V_{fb} - \frac{Q_{it}(\phi_{scr}=0)t_i}{\varepsilon_i}\right) \tag{4}$$

Where the subscript 'CV' has been added to Φ_{ms} to indicate the work function difference for the CV measurement. This indicates that CV V_{fb} measurements are more sensitive to charge closer to the insulator-silicon interface than to the metal-insulator interface (V_{fb} larger when charge resides at the insulator-silicon interface, $x_c = 0$).

Following a similar argument we can calculate the backing potential measured by the Kelvin Probe. Backing potential V_{bKP} is defined as the external potential that must be established to equalize the potential of the gate and the semiconductor. This is equivalent to the term contact potential difference (V_{CPD}) widely used in the context of surface photo-voltage measurements [19,20]. The LHS of equation (1) refers to the potential difference between the gate and the semiconductor. If the reference potential in the case of a KP measurement is given by the probe, Fig 1.b, the KP backing potential that the semiconductor takes to equalize the gate potential ($-V_g = V_{bKP}$) is:

$$V_{bKP} = -\left(\frac{\Phi_{ms}}{q} - \psi_i + \phi_{scr}\right) = \frac{\Phi_{sm}}{q} + \psi_i - \phi_{scr} \tag{5}$$

Where the change in sign indicates that V_{bKP} is compensating the sample surface potential to ensure the overall potential difference is zero, and the last term in the RHS of equation (1) has been omitted since it refers to the potential induced on the metal gate by the silicon space charge region. Φ_{sm} represents the semiconductor to metal work function difference, and ψ_i includes the air gap [3]:

$$\psi_i = -\frac{1}{K_i\varepsilon_0}\int_0^{t_i} x\rho_i(x)dx - \frac{1}{\varepsilon_0}\int_{t_i}^{t_i+t_{air}}\left(\frac{t_i}{K_i} + (x-t_i)\right)\rho_{air}(x)dx \tag{6}$$

Where K_i is the relative permittivity of the insulator and ρ_{air} the volumetric charge concentration in the air, yet a sufficiently well isolated KP instrument will produce measurements were no charge concentration exists in the air, thus the insulator potential reduces to:

$$\psi_i = -\frac{1}{K_i\varepsilon_0}\int_0^{t_i} x\rho_i(x)dx \tag{7}$$

Once again it can be assumed that all charge resides in a plane of concentration Q_i at a distance x_c from the insulator-silicon interface. Therefore $\rho_i = Q_i\,\delta(x - x_c)$. Substituting this charge profile into equation (7), the backing potential, and thus the measured charge, are given by:

$$V_{bKP} = \frac{\Phi_{smKP}}{q} - \frac{Q_i x_c}{\varepsilon_i} - \phi_{scr} \tag{8}$$

$$Q_{KP} = \frac{\varepsilon_i}{x_c}\left(\frac{\Phi_{smKP}}{q} - V_{bKP} - \phi_{scr}\right) \tag{9}$$

Where the subscript 'KP' has been added to Φ_{sm} to indicate the work function difference for the KP measurement. This calculation shows that KP measurements are more sensitive to charge at the air-insulator interface than the insulator-silicon interface. V_{bKP} is larger when $x_c = t_i$.

The concentration of charge calculated from CV and KP measurements can therefore be simplified to:

$$Q_{KP} = \frac{\varepsilon_i}{x_c}\left(\frac{\Phi_{smKP}}{q} - V_{bKP} - \phi_{scr}\right),\ Q_{CV} = \frac{\varepsilon_i}{t_i - x_c}\left(\frac{\Phi_{msCV}}{q} - V_{fb} - \frac{Q_{it}(\phi_{scr}=0)t_i}{\varepsilon_i}\right) \tag{10}$$

These two expressions can be jointly used to estimate the centroid of the charge (x_c) using combined CV and KP on the same specimen. Assuming the techniques do not inject or remove charge from the insulator-silicon structure, the total charge measured by both techniques is equal; $Q_{KP} = Q_{CV}$. x_c is then calculated from equation (10) as:

$$x_c = \frac{t_i\left(\frac{\Phi_{smKP}}{q} - V_b - \phi_{scr}\right)}{\left(\frac{\Phi_{smKP}}{q} - V_b - \phi_{scr}\right) + \left(\frac{\Phi_{msCV}}{q} - V_{fb} - \frac{Q_{it}(\phi_{scr}=0)t_i}{\varepsilon_i}\right)} \tag{11}$$

Calculating ϕ_{scr} and Q_{it} has been a well-known difficulty when using CV and KP measurements. Girisch [21] and Aberle [22] have suggested algorithms to find the concentration of interface trapped charge and surface band bending using an iterative algorithm. Fortunately, theoretical solutions for ϕ_{scr} have been deduced –e.g. in references [23] and [24]. These can be used to demonstrate that a charge concentration in the space charge region in excess of 10^{13} q/cm^2 is necessary to produce a semiconductor surface potential $|\phi_{scr}| > 0.25$ V (1 Ωcm n-type silicon), using Boltzmann statistics. The accuracy of the KP instrument used here is ~ 0.4 V, thus ϕ_{scr} can be neglected from the calculation in equation (9). Similarly, CV measurements can be used to verify that the mid-gap state density at the oxide-silicon interface is kept below 10^{12} eV^{-1}cm^{-2}, as for example reported in reference [25]. It is the states between the fermi level and intrinsic fermi level that have the greatest probability of being in the charged state and contributing to Q_{it}. For the work presented $E_F - E_i = 0.34eV$. Therefore, the number of states likely to contribute to Q_{it} if in the charged state is 3.4 x 10^{11} cm^{-2}. Assuming that only ~ 10^{11} cm^{-2} of these near mid-gap states are charged, the potential contribution of the ionized interface states is ~ 0.5 V. To a good approximation the centroid of charge is found as:

$$x_c = \frac{t_i\left(\frac{\Phi_{smKP}}{q} - V_b\right)}{\left(\frac{\Phi_{smKP}}{q} - V_b\right) + \left(\frac{\Phi_{msCV}}{q} - V_{fb}\right)} \quad (12)$$

Similar expressions have been previously used to calculate charge in electrets for example in references [26] and [27].

4. Results and discussion

4.1. KP and CV measurements of corona charge in a SiO_2-Si system

Four oxidized 1 x 1 cm^2 specimens were dehydrated, HMDS treated and deposited with corona charge. KP measurements were made on all four samples to calculate surface charge. Fig. 3 illustrates the surface charge calculated from KP measurements across specimens when annealed and/or CV measured. As-deposited corona charge was observed to reside at the air-SiO_2 interface as illustrated from the KP maps in Fig. 3.a. and b. For corona charge deposited at room temperature V_{fb} is negligible ~ 0 V, i.e. no charge has migrated into the SiO_2. CV measurements were found to interfere with the corona charge and therefore were only performed on two of the samples, Fig. 3.b,d. The mercury dot used in CV measurements was observed to affect any charge present at the dielectric surface and thus KP measurements must be made either before CV measurements or at different locations on the dielectric surface. If processing is to continue after the CV measurement, all future measurements must also be made in a different location. These measurements have shown that high temperature annealing, after corona charging, affects the location of charge within the SiO_2-Si structure. However, from the present work it is not possible to infer whether the charge that moves into the dielectric is due to the deposited corona ions themselves or due to other impurity species which may be present at the dielectric surface.

Migration of charge was conducted at 300 ˚C for 6 seconds. This lowered the V_{bKP} form ~ 11.5 V to ~ -4 V ($Q_{Air\text{-}SiO2}$ ~ 10^{11} q/cm^2). The V_{fb} is seen to increase from ~ 0 V to ~ -9 V ($Q_{Air\text{-}SiO2}$ ~ 10^{12} q/cm^2). This reduction in KP and increase in CV charge measurements indicates that the charge migrates from the air-SiO_2 interface to the SiO_2-Si interface during the anneal. From Fig. 3.d. it is also clear that the CV measurement itself affects the surface potential of the sample, even when the charge does not reside on the surface. During a CV measurement, the mercury contact on the surface of the SiO_2 is biased thus allowing charge to be transferred between the mercury and the SiO_2 surface. This charge compensates the charge present at the SiO_2 surface and is visible when conducting KP measurements. Again, this demonstrates the importance of characterizing the specimens using KP before carrying out Hg-p CV measurements.

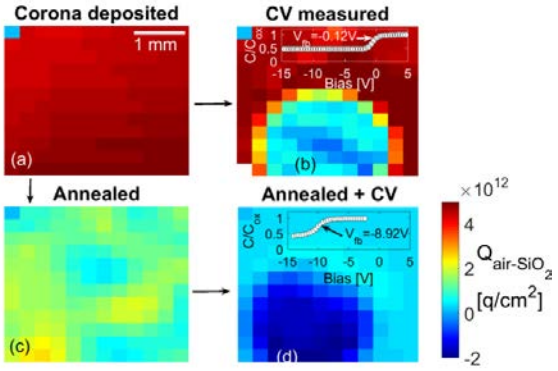

Fig. 3. Magnitude and lateral location of charge in the SiO_2-Si system after corona charge deposition and before and after a 300 ˚C anneal, (a-d) Are Kelvin Probe maps taken after different processing and measurement steps. The circular features visible in b) and d) correspond to the position where the Hg contact was made.

4.2. Location of charge after high temperature anneal

In order to confirm the location of the charge after annealing, a back etch experiment was conducted. A new, dehydrated and HMDS treated specimen was deposited with corona charge and annealed for 20 seconds at 300 ˚C. To profile the concentration of charge inside the dielectric, the SiO_2 was removed incrementally in a dilute HF solution. Fig 4 shows the flat-band voltage and equivalent charge concentration (assuming the charge resides at the SiO_2-Si interface) with respect to the oxide thickness. The oxide thickness was measured using an optical reflectometer. It was found that, during the 20 second anneal, charge migrated directly from the air-SiO_2 interface to the SiO_2-Si interface. This is demonstrated by the linear dependence of V_{fb} with t_i, shown in Fig 4. According to equation (3), this linear dependence would only occur if the charge within the dielectric remained constant, i.e. none was removed by etching the top surface. This is corroborated by the constant concentration of charge measured as a function of oxide thickness.

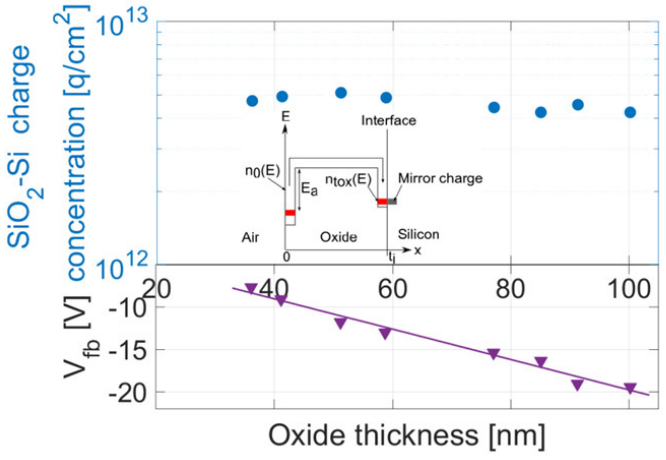

Fig 4. Charge profile using a back etch Hg-p CV flat-band voltage technique, showing charge concentration at the SiO_2-Si interface (top) and flat-band voltage (bottom) with oxide thickness.

4.3. Effective lifetime

Charge migration was also conducted on 3 x 3 cm^2 lifetime specimens with the same, corona provided, field effect passivation at both front and back oxidized surfaces. Fig. 5.a. illustrates the increase in lifetime as corona charge is applied while Fig. 5.b. illustrates the loss of charge as the specimen is annealed at 300 ˚C. The maximum lifetime achieved at $\Delta n=10^{15}$ cm^{-3} was 2.3 ms. This lifetime occurs at a surface charge concentration of ~$5x10^{12}$ q/cm^2 (V_{kp}= -26.10 V). For 200 μm thick wafers, this is equivalent to a SRV < 2.7 cm/s and J_{01} < 12 fA/cm^2 which is within the range required for high efficiency (>20%) silicon solar cells. However, the kinetic behavior of charge in the 3 x 3 cm^2 samples differed greatly from that observed in 1 x 1 cm^2 samples. The KP readings indicate that for the larger samples the charge at the surface reduces more slowly during the anneals than for smaller samples. This suggests that a size effect, most likely related to the edges of the specimen, modifies the transport of charge. One possibility is that, for the smaller specimens, the surface charge migrates relatively quickly to the edges of the specimen where it is neutralized. In addition, by comparison between samples with equal values of V_{kp}, thus Q_i, it is possible to infer from the lifetime measurements that the charge that migrates to the SiO_2-Si interface generates interface states so producing a significant reduction in effective lifetime.

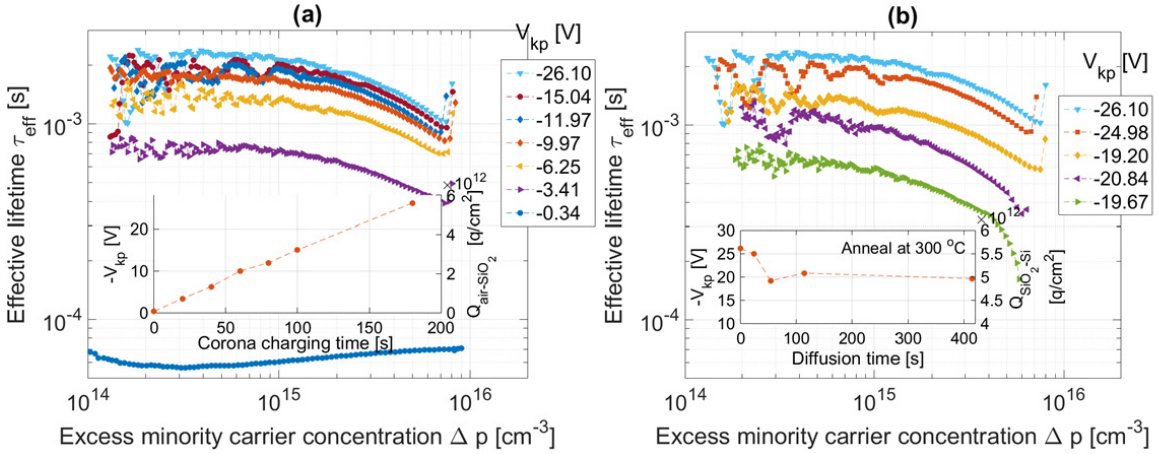

Fig. 5. Effective lifetime as function of (a) SiO_2 surface charge, (b) surface charge after annealing for times shown at 300 ˚C.

5. First order kinetic model of charge migration

In order to produce a first order kinetic model, short anneals (2-5 seconds) were conducted on a corona deposited sample and KP and CV data collected after each anneal. It was previously shown that CV measurements neutralize the surface corona charge thus each CV measurement was taken in a different location. KP measurements were all performed in a location where no previous CV measurements had been taken. The results are shown in Fig. 6. Charge location was calculated using the theory developed in Section 3, resulting in equation (12) and is presented in Table 1.

Corona charge transport into SiO_2 films was modelled using first order kinetics with a temperature dependent Arrhenius reaction rate:

$$\frac{dn(t)}{dt} + n(t)\, exp\left(-\frac{E_a}{kT}\right) = 0 \tag{13}$$

where $n(t)$ is the corona charge concentration with injection energy E_a at time t, at the air-SiO_2 interface, and $T(t)$ is the temperature as a function of time. The solution to this equation is:

$$n(t) = n(0)\, exp\left[-\int_0^t exp\left(-\frac{E_a}{kT(t')}\right) dt'\right] \tag{14}$$

For a constant temperature, the concentration of ions at the air-SiO_2 and SiO_2-Si interfaces, respectively, are:

$$n_{ao}(t) = n_0\, exp\left[-exp\left(-\frac{E_{a_{AO}}}{kT}\right) t\right] \quad \text{and} \quad n_{os}(t) = n_f\left(1 - exp\left[-exp\left(-\frac{E_{a_{OS}}}{kT}\right) t\right]\right) \tag{15}$$

where n_0 is the initial corona charge concentration, and n_f the final steady-state concentration at the SiO_2-Si interface. Migration of charge was conducted in 1 x 1 cm^2 specimens for subsequent time intervals at 300 ˚C to determine the concentration of corona charge at both interfaces as a function of anneal time, Fig. 6. The kinetics model in equation (15) was then fitted to this data, Fig. 6, and the parameters calculated as shown in Table 2.

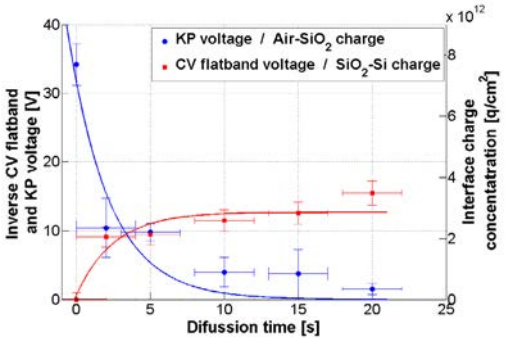

Fig. 6. Interface charge concentration as calculated from V_{kp} and V_{fb} measurements. Solid lines represent the first order kinetic model of charge migration as calculated from equation (15).

Table 1. Calculation of charge location using equation (12)

Anneal time (s)	KP (V)	CV (V)	x_c(nm from SiO2-Si interface)
0	-34.2	0	99.5
2	-10.4	-9.1	51.0
5	-9.8	-9.5	48.3
10	-4.0	-11.5	21.5
15	-3.7	-12.6	18.8
20	-1.5	-15.5	4.6

Table 2. Activation energies and interface concentrations for corona charge in a SiO_2-Si system.

Interface	Activation Energy	Steady-state charge concentration
Air-SiO2	0.0512 eV ±0.03	n_o =7.09x1012 q/cm2 ±2.7 x1012
SiO2-Si	0.0204 eV ±0.03	n_f =2.55x1012 q/cm2 ±2.7 x1012

This model indicates that injection of charge into the oxide film occurs more slowly than re-trapping at the SiO_2-Si interface. During the annealing process almost 70% of the charge ($n_0 - n_f \approx 5$ x10^{12} q/cm^2) is lost. This could be due to direct charge exchange or compensation at the SiO_2-Si interface, lateral surface leakage or evaporation off the surface. Only 2.55x10^{12} q/cm^2 was observed to have migrated to the SiO_2-Si interface, and remained charged after the anneal.

6. Conclusions

In this work, a model to estimate the centroid of charge within a dielectric using KP surface potential and CV flat-band voltage measurement is presented. A first order kinetic model is developed to describe the kinetic behavior of migration of charge in SiO_2 films after deposition of corona charge. The charge is seen to lie preferentially at the SiO_2-Si interface, suggesting that the transport mechanism is injection and/or trapping limited rather than diffusion limited. Size effects are also evident with the charge from the surface of 1 x 1 cm^2 samples seen to reduce during anneals at a much greater rate than that of 3 x 3 cm^2 samples. Lastly, very effective passivation is achieved by corona deposition on the dielectric surface and J_{01} ~ 12 fA/cm^2 is shown to be possible.

Acknowledgements

RS Bonilla is the recipient of an EPSRC (UK) Postdoctoral Research Fellowship, EP/M022196/1. PR Wilshaw acknowledges the support from EPSRC grant EP/M024911/1. Data published in this article can be downloaded from

http://ora.ox.ac.uk. KA Collet would like to thank the IET, IOP and IOM3 for travel grants to attend the Silicon PV conference. All authors are thankful to Martin Hermle and Christian Reichel at Fraunhofer ISE for provision of silicon material, and to Radka Chakalova for her extensive help in the cleanroom.

References

[1] J. Schmidt, A.G. Aberle, Easy-to-use Surface Passivation Technique for Bulk Carrier Lifetime Measurements on Silicon Wafers, Prog. Photovoltaics Res. Appl. 263 (1998) 259–263.
[2] D.K. Schroder, M.S. Fung, R.L. Verkuil, S. Pandey, W.H. Howland, M. Kleefstra, Corona-oxide-semiocnductor device characterization, Solid. State. Electron. 42 (1998) 505–512. doi:10.1016/S0038-1101(97)00206-2.
[3] R.S. Bonilla, C. Reichel, M. Hermle, P.R. Wilshaw, On the location and stability of charge in SiO2/SiNx dielectric double layers used for silicon surface passivation, J. Appl. Phys. 115 (2014) 144105. doi:10.1063/1.4871075.
[4] R.S. Bonilla, F. Woodcock, P.R. Wilshaw, Very low surface recombination velocity in n-type c-Si using extrinsic field effect passivation, J. Appl. Phys. 116 (2014) 054102.
[5] T.C. Kho, S.C. Baker-Finch, K.R. McIntosh, The study of thermal silicon dioxide electrets formed by corona discharge and rapid-thermal annealing, J. Appl. Phys. 109 (2011). doi:10.1063/1.3559260.
[6] R.S. Bonilla, P.R. Wilshaw, Stable field effect surface passivation of n-type Cz silicon, in: Energy Procedia - Proc. 3rd Silicon PV Conf., Elsevier, Hamelin, Germany, 2013: pp. 816–822. doi:10.1016/j.egypro.2013.07.351.
[7] V. Leonov, C. Hoof, M. Goedbloed, R. Schaijk, Charge injection and storage in single-layer and multilayer inorganic electrets based on SiO_2 and Si_3N_4, IEEE Trans. Dielectr. Electr. Insul. 19 (2012) 1253–1260. doi:10.1109/TDEI.2012.6259999.
[8] R.S. Bonilla, K. Collett, L. Rands, G. Martins, R. Lobo, P.R. Wilshaw, Stable, Extrinsic, Field Effect Passivation for Back Contact Silicon Solar Cells, Solid State Phenom. 242 (2015) 67–72. doi:10.4028/www.scientific.net/SSP.242.67.
[9] R.S. Bonilla, C. Reichel, M. Hermle, P.R. Wilshaw, Electric Field Effect Surface Passivation for Silicon Solar Cells, Solid State Phenom. 205-206 (2013) 346–351. http://www.scientific.net/SSP.205-206.346 (accessed October 9, 2013).
[10] L. Huamao, X. Zhongfu, S. Shaoqun, Z. Hongyan, C. Yang, Z. Jianwei, The charge dynamics of thermally wet grown SiO/sub 2/ electret by corona charging method with constant grid current, in: 9th Int. Symp. Electrets (ISE 9) Proc., IEEE, n.d.: pp. 133–138. doi:10.1109/ISE.1996.578058.
[11] W. Olthuis, P. Bergveld, On the charge storage and decay mechanism in silicon dioxide electrets, IEEE Trans. Electr. Insul. 27 (1992) 691–697. doi:10.1109/14.155784.
[12] I.D. Baikie, S. Mackenzie, P.J.Z. Estrup, J.A. Meyer, Noise and the Kelvin method, Rev. Sci. Instrum. 62 (1991) 1326–1332. doi:10.1063/1.1142494.
[13] Sinton Instruments WCT-120, (n.d.).
[14] E.H. Nicollian, J.R. Brews, MOS (Metal Oxide Semiconductor) — Physics and Technology, Wiley, New York, 1982.
[15] S.M. Sze, K.K. Ng, Physics of Semiconductor Devices, Wiley, Hoboken, New Jersey, 2007.
[16] D.K. Schroder, Semiconductor material and device characterisation, John Wiley & Sons, Inc., 2006.
[17] E.H. Snow, A.S. Grove, B.E. Deal, C.T. Sah, Ion Transport Phenomena in Insulating Films, J. Appl. Phys. 36 (1965) 1664–1673. doi:10.1063/1.1703105.
[18] B.E. Deal, M. Sklar, a. S. Grove, E.H. Snow, Characteristics of the Surface-State Charge (Qss) of Thermally Oxidized Silicon, J. Electrochem. Soc. 114 (1967) 266. doi:10.1149/1.2426565.
[19] M. Wilson, J. Lagowski, A. Savtchouk, L. Jastrzebski, J.D. Amico, D.C. Gupta, et al., COCOS (Corona Oxide Characterization of Semiconductor) Metrology : Physical Principles and Applications " COCOS (Corona Oxide Characterization of Semiconductor) Metrology : Physical Principles and Applications ," Gate Dielectric Integrity : Material , (2000) 74–90.
[20] M. Wilson, COCOS (corona oxide characterization of semiconductor) non-contact metrology for gate dielectrics, AIP Conf. Proc. 550 (2001) 220–225. doi:10.1063/1.1354401.
[21] R.B.M. Girisch, R.P. Mertens, R.F. De Keersmaecker, Determination of Si-Sio//2 Interface Recombination Parameters Using a Gate-Controlled Point-Junction Diode Under Illumination., IEEE Trans. Electron Devices. 35 (1988) 203–222. doi:10.1109/16.2441.
[22] A.G. Aberle, S. Glunz, W. Warta, Impact of illumination level and oxide parameters on Shockley-Read-Hall recombination at the Si-SiO2 interface, J. Appl. Phys. 71 (1992) 4422–4431. doi:10.1063/1.350782.
[23] W. Mönch, Semiconductor Surfaces and Interfaces, 3rd Editio, Springer, 2001.
[24] a. S. Grove, D.J. Fitzgerald, Characteristics of surface space-charge regions under non-equilibrium conditions, IEEE Trans. Electron Devices. 13 (1966) 783–806. doi:10.1109/T-ED.1966.15779.
[25] S.W. Glunz, D. Biro, S. Rein, W. Warta, Field-effect passivation of the SiO2-Si interface, J. Appl. Phys. 86 (1999) 683. doi:10.1063/1.370784.
[26] R. Kressmann, G.M. Sessler, P. Günther, Space-charge electrets, IEEE Trans. Dielectr. Electr. Insul. 3 (1996) 607–623. doi:10.1109/94.544184.
[27] P. Gunther, Z. Xia, Transport of detrapped charges in thermally wet grown SiO2 electrets, J. Appl. Phys. 74 (1993) 7269–7274. doi:10.1063/1.354992.